Determination of energy loss and efficiency for the low power steam turbine and each of its segments

Mrzljak Vedran[1], Prpić-Oršić Jasna[1], Poljak Igor[2], Anđelić Nikola[1]
[1]Faculty of Engineering, University of Rijeka, Vukovarska 58, 51000 Rijeka, Croatia
[2]Department of maritime sciences, University of Zadar, Mihovila Pavlinovića 1, 23000 Zadar, Croatia
E-mail: vedran.mrzljak@riteh.hr, jasna.prpic-orsic@riteh.hr, ipoljak1@unizd.hr, nandelic@riteh.hr

Abstract: *In this paper is performed energy analysis of the whole low power steam turbine as well as energy analysis of all the turbine segments. Analysis of the whole turbine resulted with energy loss of 14642.48 kW and energy efficiency of 75.01%, what is in range with similar comparable low power steam turbines. Energy analysis of the turbine segments presents a different conclusion than the energy analysis of the whole turbine. The fifth turbine segment (S5) has unacceptable high energy loss and unacceptable low energy efficiency (energy loss of 6785.93 kW and energy efficiency of 26.87%), so it should be repaired as soon as possible. This comparison show that proper energy analysis of turbine parts (segments) can detect the precise location of the problems during the turbine operation. Such analysis can be very helpful for the engineers because it allows detection not only the problematic components in the power plant, but also allows detection of the problematic parts of a component.*

KEYWORDS*: LOW POWER STEAM TURBINE, TURBINE SEGMENTS, ENERGY LOSS, ENERGY EFFICIENCY*

1. Introduction

The most of electric power worldwide is produced by steam turbines. For the high power steam turbines, which are constituent parts of many various power plants, the dominant function is to transform high amount of mechanical energy into the electric energy [1-3]. Nowadays, mentioned high power steam turbines are composed of several cylinders, while each cylinder consists of many turbine stages [4, 5].

Low power steam turbines, in comparison to high power ones, are not so dominantly used worldwide. However, they have its functions in many systems, plants and processes. They can be found on ships for propulsion or for electric power production [6-8], in cogeneration power plants [9], in many processes for driving of various pumps or compressors [10, 11], in many industrial and complex power plants [12], etc.

In this paper is performed energy analysis of one selected low power steam turbine. Firstly was performed energy analysis of the whole turbine, after which is performed an energy analysis of all turbine segments (analyzed turbine has five steam extractions and six segments). The energy analysis of turbine segments can detect problems during operation in any turbine part (segment), while the analysis of the whole turbine cannot detect such problems.

2. Analyzed low power steam turbine description

The analyzed steam turbine operates as a part of steam power plant in an iron and steel facility [13]. The turbine has one cylinder which drives an electric generator, as presented in Fig. 1. Steam delivered to the turbine inlet (operating point 1, Fig. 1) is produced in a steam generator [14]. The turbine has five steam extractions – first two extractions (operating points 2 and 3, Fig. 1) delivers a certain steam mass flow rate to high pressure feed water heating system, one extraction (operating point 4, Fig. 1) delivers a certain steam mass flow rate to deaerator and last two extractions (operating points 5 and 6, Fig. 1) delivers a certain steam mass flow rate to low pressure condensate heating system. A steam mass flow rate, which remains after all extractions (operating point 7, Fig. 1) is delivered to the main condenser for condensation [15].

All seven operating points of the analyzed turbine represent places where steam operating parameters (steam pressure, temperature and mass flow rate) should be measured inside a power plant to get all the required data for the energy analysis. Measured data will define real (polytropic) steam expansion process inside the observed turbine.

Along with energy analysis of the whole observed turbine, in this paper will also be performed energy analysis of the turbine segments. Turbine segments are defined between operating points in Fig. 1 and marked from S1 to S6. Dividing of the turbine cylinder into the segments will allow calculation of energy efficiency and loss in each segment. In such way, detection of potential problems (high loss and low efficiency) inside each segment can be easily conducted.

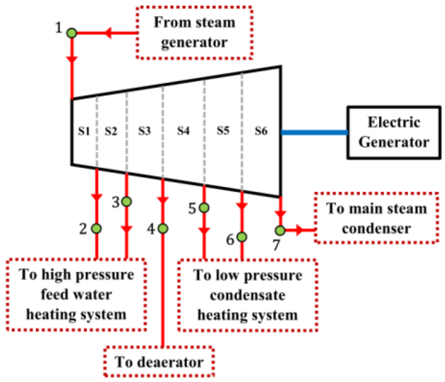

Fig. 1. *Scheme of the observed steam turbine as well as operating points required for the energy analysis and markings of turbine segments (S1 – S6)*

Measurement results in each operating point from Fig. 1 defines real (polytropic) steam expansion process presented in Fig. 2 with blue line and operating points 1-2-3-4-5-6-7. Operating points from Fig. 2 are defined in relation to markings from Fig. 1.

Energy analysis of any steam turbine or its segments, is based on the comparison of real (polytropic) and ideal (isentropic) steam expansion processes [16]. Ideal (isentropic) steam expansion process is the process between the same pressures and by using the same steam mass flow rates as in real (polytropic) expansion process, but assuming always the same steam specific entropy [17]. In Fig. 2, ideal (isentropic) steam expansion process for the whole analyzed turbine is marked with dashed red line and with operating point's 1-2is-3is-4is-5is-6is-7is. Steam operating parameters for the ideal expansion process are obtained mathematically. Dark red arrows in Fig. 2 represent steam extractions.

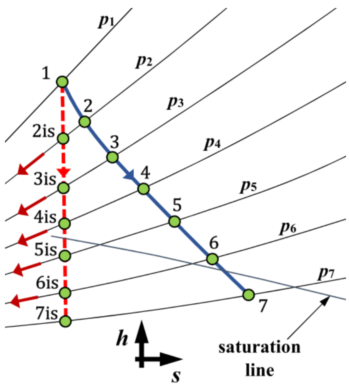

Fig. 2. *Specific enthalpy-specific entropy (h-s) diagram of real (polytropic) and ideal (isentropic) steam expansion processes while observing the whole turbine*

Energy analysis of the observed steam turbine segments cannot be performed in a same way and by using the same *h-s* diagram as for the whole turbine (Fig. 2).

Firstly, it should be stated that real (polytropic) steam expansion remains the same, with a same operating points, regardless of the fact if the whole turbine or turbine segments were observed, Fig. 3. When observing turbine segments, ideal (isentropic) expansion process begins at the inlet of each segment and lasts till reaching pressure at the segment outlet, Fig. 3. The main reason why for the turbine segments cannot be used *h-s* diagram of the whole turbine (Fig. 2) is fact that the isobars in that diagram are not parallel. The interval between two isobars increases during the increase in steam specific entropy. Therefore, for some turbine segments in Fig. 2 can be obtained that specific work in ideal expansion is lower than specific work in real expansion.

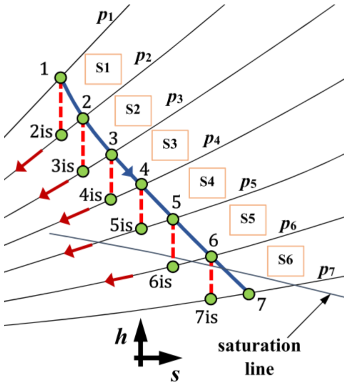

Fig. 3. *Specific enthalpy-specific entropy (h-s) diagram of real (polytropic) and ideal (isentropic) steam expansion processes while observing the turbine segments*

3. Energy analysis equations

3.1. Standard energy equations and balances valid for any component

In comparison to exergy analysis, which is based on the second law of thermodynamics and dependable on the conditions of the ambient in which component or system operates [18, 19], energy analysis is based on the first law of thermodynamics and is not dependable on the ambient conditions [20, 21]. Standard energy balance equation (disregarding potential and kinetic energies) is [22]:

$$\dot{Q}_{\mathrm{IN}} - \dot{Q}_{\mathrm{OUT}} + P_{\mathrm{IN}} - P_{\mathrm{OUT}} + \sum \dot{E}n_{\mathrm{IN}} - \sum \dot{E}n_{\mathrm{OUT}} = 0, \tag{1}$$

where $\dot{Q}$ is an energy transfer by heat, P is mechanical power, index IN denotes inlet (input) and index OUT denotes outlet (output). The last undefined variable from Eq. (1) is a total energy power of operating fluid flow ($\dot{E}n$) which can be defined according to [23] as:

$$\dot{E}n = \dot{m} \cdot h, \tag{2}$$

where $\dot{m}$ is operating fluid mass flow rate and h is operating fluid specific enthalpy. During standard operation (valid for any component or a system) fluid mass flow rate leakage did not occur, therefore the valid mass flow rate balance is [24]:

$$\sum \dot{m}_{\mathrm{IN}} = \sum \dot{m}_{\mathrm{OUT}}. \tag{3}$$

The standard energy efficiency equation is [25]:

$$\eta_{\mathrm{EN}} = \frac{\text{CUMULATIVE ENERGY OUTLET (OUTPUT)}}{\text{CUMULATIVE ENERGY INLET (INPUT)}}. \tag{4}$$

Equations and balances presented in this sub-section are (and must be) fulfilled also in the energy analysis of the whole observed steam turbine and each turbine segment.

3.2. Energy analysis equations of observed low power steam turbine and its segments

Energy analysis of the whole turbine is based on the steam expansion processes presented in Fig. 2, while the energy analysis of the turbine segments is based on the steam expansion processes presented in Fig. 3. For the whole turbine energy analysis equations are presented independently, while for the turbine segments energy analysis equations are presented in Table 1.

Energy analysis of the whole turbine (WT)

- Real (polytropic) power:

$$P_{\mathrm{RE,WT}} = \dot{m}_1 \cdot (h_1 - h_2) + (\dot{m}_1 - \dot{m}_2) \cdot (h_2 - h_3) + (\dot{m}_1 - \dot{m}_2 - \dot{m}_3) \cdot (h_3 - h_4) + (\dot{m}_1 - \dot{m}_2 - \dot{m}_3 - \dot{m}_4) \cdot (h_4 - h_5) + (\dot{m}_1 - \dot{m}_2 - \dot{m}_3 - \dot{m}_4 - \dot{m}_5) \cdot (h_5 - h_6) + (\dot{m}_1 - \dot{m}_2 - \dot{m}_3 - \dot{m}_4 - \dot{m}_5 - \dot{m}_6) \cdot (h_6 - h_7). \tag{5}$$

- Ideal (isentropic) power:

$$P_{\mathrm{ID,WT}} = \dot{m}_1 \cdot (h_1 - h_{2\mathrm{is}}) + (\dot{m}_1 - \dot{m}_2) \cdot (h_{2\mathrm{is}} - h_{3\mathrm{is}}) + (\dot{m}_1 - \dot{m}_2 - \dot{m}_3) \cdot (h_{3\mathrm{is}} - h_{4\mathrm{is}}) + (\dot{m}_1 - \dot{m}_2 - \dot{m}_3 - \dot{m}_4) \cdot (h_{4\mathrm{is}} - h_{5\mathrm{is}}) + (\dot{m}_1 - \dot{m}_2 - \dot{m}_3 - \dot{m}_4 - \dot{m}_5) \cdot (h_{5\mathrm{is}} - h_{6\mathrm{is}}) + (\dot{m}_1 - \dot{m}_2 - \dot{m}_3 - \dot{m}_4 - \dot{m}_5 - \dot{m}_6) \cdot (h_{6\mathrm{is}} - h_{7\mathrm{is}}). \tag{6}$$

- Energy loss:

$$\dot{E}n_{\mathrm{L,WT}} = P_{\mathrm{ID,WT}} - P_{\mathrm{RE,WT}}. \tag{7}$$

- Energy efficiency:

$$\eta_{\mathrm{EN,WT}} = \frac{P_{\mathrm{RE,WT}}}{P_{\mathrm{ID,WT}}}. \tag{8}$$

Energy analysis of the turbine segments

Table 1. *Energy analysis equations of the turbine segments*

SEG.	Real (polytropic) power	Eq.	Ideal (isentropic) power	Eq.
S1	$P_{\mathrm{RE,S1}} = \dot{m}_1 \cdot (h_1 - h_2)$	(9)	$P_{\mathrm{ID,S1}} = \dot{m}_1 \cdot (h_1 - h_{2\mathrm{is}})$	(15)
S2	$P_{\mathrm{RE,S2}} = (\dot{m}_1 - \dot{m}_2) \cdot (h_2 - h_3)$	(10)	$P_{\mathrm{ID,S2}} = (\dot{m}_1 - \dot{m}_2) \cdot (h_2 - h_{3\mathrm{is}})$	(16)
S3	$P_{\mathrm{RE,S3}} = (\dot{m}_1 - \dot{m}_2 - \dot{m}_3) \cdot (h_3 - h_4)$	(11)	$P_{\mathrm{ID,S3}} = (\dot{m}_1 - \dot{m}_2 - \dot{m}_3) \cdot (h_3 - h_{4\mathrm{is}})$	(17)
S4	$P_{\mathrm{RE,S4}} = (\dot{m}_1 - \dot{m}_2 - \dot{m}_3 - \dot{m}_4) \cdot (h_4 - h_5)$	(12)	$P_{\mathrm{ID,S4}} = (\dot{m}_1 - \dot{m}_2 - \dot{m}_3 - \dot{m}_4) \cdot (h_4 - h_{5\mathrm{is}})$	(18)
S5	$P_{\mathrm{RE,S5}} = (\dot{m}_1 - \dot{m}_2 - \dot{m}_3 - \dot{m}_4 - \dot{m}_5) \cdot (h_5 - h_6)$	(13)	$P_{\mathrm{ID,S5}} = (\dot{m}_1 - \dot{m}_2 - \dot{m}_3 - \dot{m}_4 - \dot{m}_5) \cdot (h_5 - h_{6\mathrm{is}})$	(19)
S6	$P_{\mathrm{RE,S6}} = (\dot{m}_1 - \dot{m}_2 - \dot{m}_3 - \dot{m}_4 - \dot{m}_5 - \dot{m}_6) \cdot (h_6 - h_7)$	(14)	$P_{\mathrm{ID,S6}} = (\dot{m}_1 - \dot{m}_2 - \dot{m}_3 - \dot{m}_4 - \dot{m}_5 - \dot{m}_6) \cdot (h_6 - h_{7\mathrm{is}})$	(20)
SEG.	**Energy loss**	**Eq.**	**Energy efficiency**	**Eq.**
S1	$\dot{E}n_{\mathrm{L,S1}} = P_{\mathrm{ID,S1}} - P_{\mathrm{RE,S1}}$	(21)	$\eta_{\mathrm{EN,S1}} = \frac{P_{\mathrm{RE,S1}}}{P_{\mathrm{ID,S1}}}$	(27)
S2	$\dot{E}n_{\mathrm{L,S2}} = P_{\mathrm{ID,S2}} - P_{\mathrm{RE,S2}}$	(22)	$\eta_{\mathrm{EN,S2}} = \frac{P_{\mathrm{RE,S2}}}{P_{\mathrm{ID,S2}}}$	(28)
S3	$\dot{E}n_{\mathrm{L,S3}} = P_{\mathrm{ID,S3}} - P_{\mathrm{RE,S3}}$	(23)	$\eta_{\mathrm{EN,S3}} = \frac{P_{\mathrm{RE,S3}}}{P_{\mathrm{ID,S3}}}$	(29)
S4	$\dot{E}n_{\mathrm{L,S4}} = P_{\mathrm{ID,S4}} - P_{\mathrm{RE,S4}}$	(24)	$\eta_{\mathrm{EN,S4}} = \frac{P_{\mathrm{RE,S4}}}{P_{\mathrm{ID,S4}}}$	(30)
S5	$\dot{E}n_{\mathrm{L,S5}} = P_{\mathrm{ID,S5}} - P_{\mathrm{RE,S5}}$	(25)	$\eta_{\mathrm{EN,S5}} = \frac{P_{\mathrm{RE,S5}}}{P_{\mathrm{ID,S5}}}$	(31)
S6	$\dot{E}n_{\mathrm{L,S6}} = P_{\mathrm{ID,S6}} - P_{\mathrm{RE,S6}}$	(26)	$\eta_{\mathrm{EN,S6}} = \frac{P_{\mathrm{RE,S6}}}{P_{\mathrm{ID,S6}}}$	(32)

4. Steam operating parameters for the analysis

In each operating point from Fig. 1 required steam operating parameters for real expansion process are found in [13] and presented in Table 2. Steam specific enthalpy and steam specific entropy are calculated from known steam temperature and pressure in each operating point (Fig. 1) by using NIST-REFPROP 9.0 software [26].

Steam operating parameters for ideal (isentropic) steam expansion process, according to Fig. 2, required in the energy analysis of the whole steam turbine, are presented in Table 3. In the energy analysis of turbine segments, according to Fig. 3, steam specific enthalpies in each required operating point for the ideal (isentropic) steam expansion process are presented in Table 4.

Table 2. *Steam operating parameters of the real (polytropic) steam expansion process*

O.P.*	Temperature (°C)	Pressure (kPa)	Mass flow rate (kg/s)	Specific enthalpy (kJ/kg)	Specific entropy (kJ/kg·K)
1	532.00	8800	51.97	3469.6	6.7742
2	356.40	2363	2.27	3144.5	6.8952
3	304.70	1501	3.19	3048.6	6.9376
4	244.10	887	2.77	2934.4	6.9631
5	125.60	236	3.13	2714.0	7.0721
6	85.70	59	2.78	2652.6	7.5380
7	52.55	14	37.83	2524.5	7.8123

* O.P. = Operating Point (according to Fig. 1)

Table 3. *Steam operating parameters of the ideal (isentropic) steam expansion process for the whole turbine (Fig. 2)*

O.P.*	Pressure (kPa)	Mass flow rate (kg/s)	Specific entropy-isentropic (kJ/kg·K)	Specific enthalpy-isentropic (kJ/kg)
1	8800	51.97	6.7742	3469.6
2is	2363	2.27	6.7742	3070.3
3is	1501	3.19	6.7742	2957.5
4is	887	2.77	6.7742	2840.7
5is	236	3.13	6.7742	2595.2
6is	59	2.78	6.7742	2378.6
7is	14	37.83	6.7742	2186.4

* O.P. = Operating point (according to Fig. 2)

Table 4. *Steam operating parameters of the ideal (isentropic) steam expansion process for the turbine segments (Fig. 3)*

O.P.*	Pressure (kPa)	Mass flow rate (kg/s)	Specific entropy-isentropic (kJ/kg·K)	Specific enthalpy-isentropic (kJ/kg)
1	8800	51.97	6.7742	3469.6
2is	2363	2.27	6.7742	3070.3
3is	1501	3.19	6.8952	3024.3
4is	887	2.77	6.9376	2921.3
5is	236	3.13	6.9631	2670.6
6is	59	2.78	7.0721	2485.5
7is	14	37.83	7.5380	2435.2

* O.P. = Operating point (according to Fig. 3)

5. Results and discussion

Energy analysis of the whole observed low power steam turbine resulted with turbine real (polytropic) power equal to 43952.89 kW and ideal (isentropic) power equal to 58595.37 kW, Fig. 4. Energy loss of the whole turbine is equal to 14642.48 kW. Energy efficiency of the whole analyzed turbine is 75.01%. Such energy efficiency of the whole turbine is in range with other similar low power steam turbines from the literature [27]. Therefore, from the energy analysis of the whole observed turbine can be concluded that energy loss and energy efficiency are in range with other comparable low power steam turbines and that there is no obvious problems in operation.

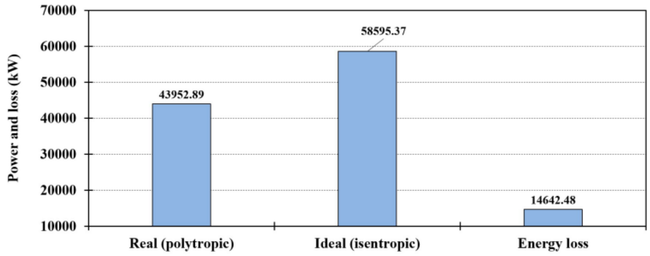

Fig. 4. *Real (polytropic) and ideal (isentropic) power as well as energy loss of the whole analyzed turbine*

Real (polytropic) and ideal (isentropic) power for each segment of the observed steam turbine are presented in Fig. 5. Analysis of obtained results for each segment leads to conclusion that the highest power (regardless if it is ideal or real) is developed in the first turbine segment (S1). Also, in S1 can be expected relatively high energy loss due to the highest steam pressure and temperature (much higher in comparison to other turbine segments). Segments two, three and four (S2, S3 and S4) will have low energy losses, because the difference between ideal and real power is small. For the last turbine segment (S6) is expected that the energy loss will be high, because only that segment (in comparison to all the others) operates with wet steam, Fig. 2 and Fig. 3. When observing fifth turbine segment (S5) it can be seen the highest difference between ideal and real power (in comparison to all the other turbine segments), Fig. 5. As S5 operates with superheated steam which did not consist of water droplets, the only reason for such operation of S5 can be found in some problems, the occurrence of the unexpected additional losses, degradation of turbine blades, etc.

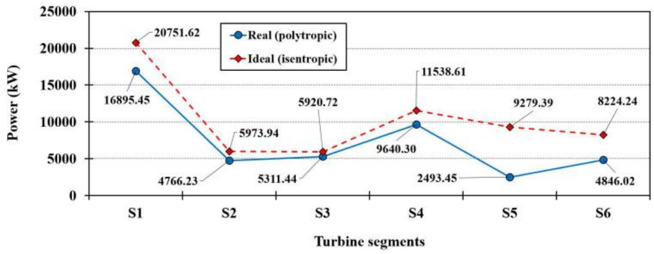

Fig. 5. *Real (polytropic) and ideal (isentropic) power of the turbine segments*

As mentioned before, the first segment of the observed steam turbine (S1) has high energy loss due to high steam pressure and temperature, Fig. 6. Slightly lower energy loss than in S1 can be observed in the last turbine segment (S6) due to operation with wet steam. Segments two, three and four (S2, S3 and S4) have low energy loss. The highest energy loss of all segments from the observed turbine can be seen in the fifth segment (S5), which can be explained only by some evident problems in that segment operation.

The energy efficiency of the first four turbine segments is reasonably high (around 80% or higher). The last turbine segment (S6) has an energy efficiency equal to 58.92%, what is also expected. Fifth turbine segment (S5) has an energy efficiency equal to 26.87%, what can be explained only by evident problems in operation.

Finally, it can be concluded that energy analysis of the turbine segments gives the proper presentation of turbine parts operation and can detect segments in which occur unexpected losses (as in the case of the analyzed turbine). Energy analysis of the whole turbine cannot detect such details.

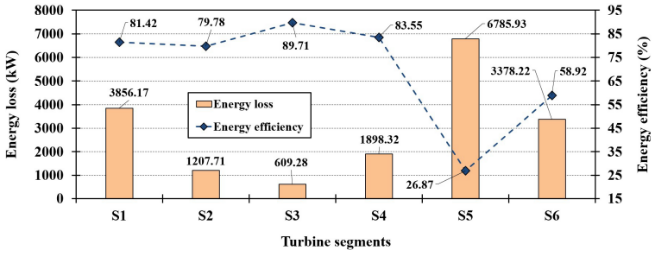

***Fig. 6.** Energy loss and energy efficiency of the turbine segments*

Further research of the observed steam turbine and its segments will be performed by the application of many artificial intelligence methods and processes [28-31]. It can be expected that all of the further analyzes will result with a same conclusion that the fifth turbine segment (S5) should be repaired as soon as possible.

6. Conclusions

In this paper is performed analysis of energy loss and energy efficiency (energy analysis) of low power steam turbine which operates in an iron and steel facility. The energy analysis is firstly performed for the whole turbine, after which follows the analysis for all turbine segments. The main conclusions are:

- Energy analysis of the whole turbine resulted with energy loss equal to 14642.48 kW and with energy efficiency of 75.01%. Calculated energy loss and efficiency of the whole turbine did not show any potential problem in operation – such energy efficiency and loss are in the range with other comparable low power steam turbines.
- Energy analysis of turbine segments resulted with a fact that the fifth turbine segment (S5) has unacceptable high energy loss and unacceptable low energy efficiency (energy loss of 6785.93 kW and energy efficiency of 26.87%). Therefore, fifth turbine segment (S5) should be repaired as soon as possible.
- Presented analysis can be very helpful for the engineers in exploitation because it allows detection not only the problematic components in the power plant, but also allows detection of problematic parts of the components.

7. Acknowledgment

This research has been supported by the Croatian Science Foundation under the project IP-2018-01-3739, CEEPUS network CIII-HR-0108, European Regional Development Fund under the grant KK.01.1.1.01.0009 (DATACROSS), project CEKOM under the grant KK.01.2.2.03.0004, CEI project “COVIDAi” (305.6019-20), University of Rijeka scientific grant uniri-tehnic-18-275-1447 and University of Rijeka scientific grant uniri-tehnic-18-18-1146.

8. References

[1] Zhao, Z., Su, S., Si, N., Hu, S., Wang, Y., Xu, J., ... & Xiang, J. (2017). *Exergy analysis of the turbine system in a 1000 MW double reheat ultra-supercritical power plant.* Energy, 119, 540-548. (doi:10.1016/j.energy.2016.12.072)

[2] Lorencin, I., Anđelić, N., Mrzljak, V., & Car, Z. (2019). *Genetic Algorithm Approach to Design of Multi-Layer Perceptron for Combined Cycle Power Plant Electrical Power Output Estimation*. Energies, 12(22), 4352. (doi:10.3390/en12224352)

[3] Elhelw, M., Al Dahma, K. S., & el Hamid Attia, A. (2019). *Utilizing exergy analysis in studying the performance of steam power plant at two different operation mode*. Applied Thermal Eng., 150, 285-293. (doi:10.1016/j.applthermaleng.2019.01.003)

[4] Kostyuk, A., & Frolov, V. (1988). *Steam and gas turbines*. Mir Publishers.

[5] Tanuma, T. (Ed.). (2017). *Advances in Steam Turbines for Modern Power Plants*. Woodhead Publishing.

[6] Mrzljak, V., Poljak, I., & Prpić-Oršić, J. (2019). *Exergy analysis of the main propulsion steam turbine from marine propulsion plant*. Shipbuilding, 70(1), 59-77. (doi:10.21278/brod70105)

[7] Koroglu, T., & Sogut, O. S. (2018). *Conventional and advanced exergy analyses of a marine steam power plant*. Energy, 163, 392-403. (doi:10.1016/j.energy.2018.08.119)

[8] Mrzljak, V., Senčić, T., & Žarković, B. (2018). *Turbogenerator steam turbine variation in developed power: Analysis of exergy efficiency and exergy destruction change*. Modelling and Simulation in Engineering, 2018. (doi:10.1155/2018/2945325)

[9] Burin, E. K., Vogel, T., Multhaupt, S., Thelen, A., Oeljeklaus, G., Görner, K., & Bazzo, E. (2016). *Thermodynamic and economic evaluation of a solar aided sugarcane bagasse cogeneration power plant.* Energy, 117, 416-428. (doi:10.1016/j.energy.2016.06.071)

[10] Mrzljak, V. (2018). *Low power steam turbine energy efficiency and losses during the developed power variation*. Tehnički glasnik, 12(3), 174-180. (doi:10.31803/tg-20180201002943)

[11] Mrzljak, V., Prpić-Oršić, J., & Poljak, I. (2018). *Energy Power Losses and Efficiency of Low Power Steam Turbine for the Main Feed Water Pump Drive in the Marine Steam Propulsion System*. Pomorski zbornik, 54(1), 37-51. (doi:10.18048/2018.54.03)

[12] Hafdhi, F., Khir, T., Yahyia, A. B., & Brahim, A. B. (2015). *Energetic and exergetic analysis of a steam turbine power plant in an existing phosphoric acid factory*. Energy Conversion and Manag., 106, 1230-1241. (doi:10.1016/j.enconman.2015.10.044)

[13] Yılmaz, K., Kayfeci, M., & Keçebaş, A. (2019). *Thermodynamic evaluation of a waste gas-fired steam power plant in an iron and steel facility using enhanced exergy analysis*. Energy, 169, 684-695. (doi:10.1016/j.energy.2018.12.007)

[14] Mrzljak, V., Poljak, I., & Medica-Viola, V. (2017). *Dual fuel consumption and efficiency of marine steam generators for the propulsion of LNG carrier*. Applied Thermal Engineering, 119, 331-346. (doi:10.1016/j.applthermaleng.2017.03.078)

[15] Škopac, L., Medica-Viola, V., & Mrzljak, V. (2020). *Selection Maps of Explicit Colebrook Approximations according to Calculation Time and Precision*. Heat Transfer Engineering, 1-15. (doi:10.1080/01457632.2020.1744248)

[16] Elčić, Z. (1995). *Steam turbines*. ABB, Karlovac, National and University Library Zagreb.

[17] Moran, M. J., Shapiro, H. N., Boettner, D. D., & Bailey, M. B. (2010). *Fundamentals of engineering thermodynamics*. John Wiley & Sons.

[18] Szargut, J. (2005). *Exergy method: technical and ecological applications* (Vol. 18). WIT press.

[19] Lorencin, I., Anđelić, N., Mrzljak, V., & Car, Z. (2019). *Exergy analysis of marine steam turbine labyrinth (gland) seals*. Pomorstvo, 33(1), 76-83. (doi:10.31217/p.33.1.8)

[20] Kanoğlu, M., Çengel, Y. A., & Dinçer, İ. (2012). *Efficiency evaluation of energy systems*. Springer.

[21] Kocijel, L., Poljak, I., Mrzljak, V., & Car, Z. (2020). *Energy Loss Analysis at the Gland Seals of a Marine Turbo-Generator Steam Turbine*. Tehnički glasnik, 14(1), 19-26. (doi:10.31803/tg-20191031094436)

[22] Mrzljak, V., Blecich, P., Anđelić, N., & Lorencin, I. (2019). *Energy and Exergy Analyses of Forced Draft Fan for Marine Steam Propulsion System during Load Change*. Journal of Marine Sci. and Eng., 7(11), 381. (doi:10.3390/jmse7110381)

[23] Medica-Viola, V., Mrzljak, V., Anđelić, N., & Jelić, M. (2020). *Analysis of Low-Power Steam Turbine With One Extraction for Marine Applications*. NAŠE MORE, 67(2), 87-95. (doi:10.17818/NM/2020/2.1)

[24] Aljundi, I. H. (2009). *Energy and exergy analysis of a steam* *power plant in Jordan*. Applied Thermal Eng., 29(2-3), 324-328. (doi:10.1016/j.applthermaleng.2008.02.029)

[25]Medica-Viola, V., Baressi Šegota, S., Mrzljak, V., & Štifanić, D. (2020). *Comparison of conventional and heat balance based energy analyses of steam turbine*. Pomorstvo, 34(1), 74-85. (doi:10.31217/p.34.1.9)

[26]Lemmon, E. W., Huber, M. L., & McLinden, M. O. (2010). NIST Standard Reference Database 23, *Reference Fluid Thermodynamic and Transport Properties (REFPROP)*, version 9.0, National Institute of Standards and Technology. R1234yf. fld file dated December, 22, 2010.

[27]Mrzljak, V., & Poljak, I. (2019). *Energy Analysis of Main Propulsion Steam Turbine from Conventional LNG Carrier at Three Different Loads*. NAŠE MORE, 66(1), 10-18. (doi:10.17818/NM/2019/1.2)

[28]Lorencin, I., Anđelić, N., Mrzljak, V., & Car, Z. (2019). *Marine Objects Recognition Using Convolutional Neural Networks*. NAŠE MORE, 66(3), 112-119. (doi:10.17818/NM/2019/3.3)

[29]Baressi Šegota, S., Lorencin, I., Ohkura, K., & Car, Z. (2019). *On the Traveling Salesman Problem in Nautical Environments: an Evolutionary Computing Approach to Optimization of Tourist Route Paths in Medulin*, Croatia. Pomorski zbornik, 57(1), 71-87. (doi:10.18048/2019.57.05)

[30] Car, Z., Baressi Šegota, S., Anđelić, N., Lorencin, I., & Mrzljak, V. (2020). *Modeling the Spread of COVID-19 Infection Using a Multilayer Perceptron*. Computational and Mathematical Methods in Medicine, 2020. (doi:10.1155/2020/5714714)

[31]Baressi Šegota, S., Lorencin, I., Anđelić, N., Mrzljak, V., & Car, Z. (2020). *Improvement of Marine Steam Turbine Conventional Exergy Analysis by Neural Network Application*. Journal of Marine Science and Engineering, 8(11), 884. (doi:10.3390/jmse8110884)